Journal of Catalysis 265 (2009) 19–25

Contents lists available at ScienceDirect

Journal of Catalysis

journal homepage: www.elsevier.com/locate/jcat

Design of highly active and chemoselective bimetallic gold–platinum hydrogenation catalysts through kinetic and isotopic studies

Pedro Serna, Patricia Concepción, Avelino Corma *

Instituto de Tecnología Química, UPV-CSIC, Universidad Politécnica de Valencia, Avda. de los Naranjos s/n, 46022 Valencia, Spain

ARTICLE INFO

Article history:
Received 21 January 2009
Revised 3 April 2009
Accepted 3 April 2009
Available online 8 May 2009

Keywords:
Hydrogenation of nitroaromatics
Bimetallic gold catalysts
Chemoselective hydrogenations
kinetics of hydrogenation reactions

ABSTRACT

Kinetic model for the chemoselective hydrogenation of nitroaromatic compounds on Au/TiO_2 has been established by combining the Hougen–Watson formalism and isotopic studies. It has been found that, with this catalyst, the controlling step corresponds to the dissociation of H_2 on gold atoms of low coordination. Taking this into account, a new bimetallic $Au@Pt/TiO_2$ solid has been prepared that, when optimised, increases the rate of H_2 dissociation while preserving high chemoselectivity. The resultant catalyst is the most effective catalyst reported, up to now, for hydrogenating nitroaromatic compounds in the presence of other sensitive functionalities.

1. Introduction

The discovery of gold catalysts for the production of substituted anilines and related derivatives has opened up new possibilities around the chemistry of nitrogenated compounds [1,2]. Regarding the hydrogenation of nitroaromatic compounds, the use of synthesis procedures to create well-dispersed metal, and especially gold nanoparticles, onto the appropriated support allows designing processes where inefficient stoichiometric reducing agents such as sodium hydrosufide [3], iron [4], tin [5] or zinc in ammonium hydroxide [6], or catalysts based on $Pb–Pt/CaCO_3$ with iron salts in solution or $H_3PO_2–Pt/C$ with vanadium salts in solution [7,8] can be substituted by more efficient and greener catalytic systems. In this sense, gold can be especially sensitive to discriminate different functional groups in poly-substituted compounds, offering an alternative for manufacturing complex chemicals and fine chemicals [1,9–20]. Unfortunately, in the case of the hydrogenation of substituted nitroaromatics to the corresponding anilines, the activity of the Au/TiO_2 catalyst could be too low for practical applications [2]. The challenge was then to increase the catalyst activity while preserving its high chemoselectivity.

When attempting to design a more efficient catalyst, it is highly desirable to know the molecular mechanism and the catalytic active sites involved. A contribution to this has been recently presented [21], in which the activation of the nitroaromatic compound was shown to take place at Au/Ti boundaries, and the reduction process occurs on the gold nanoparticle after the dissociation of H_2. Thus, in order to design a more active catalyst one should know if the controlling step of the reaction corresponds to the adsorption of the substituted nitroaromatic compound through the nitro group, to the rate of H_2 dissociation on gold atoms or to the surface reaction between the adsorbed nitro compound and the dissociated H_2. It is clear that depending on the rate-controlling step, one will take different actions to modify the characteristics of the catalyst to improve its activity.

In the present work, a kinetic and isotopic study has been carried out, which has allowed finding that the rate-controlling step for the hydrogenation of substituted nitroaromatics on Au/TiO_2 corresponds to the dissociation of H_2 on the gold nanoparticles. Taking this into account, a new optimised bimetallic $Au–Pt/TiO_2$ catalyst has been prepared. Thanks to the presence of Pt, the amount of dissociated H_2 available on the catalyst surface increases, resulting in a solid that is almost one order of magnitude more active than the corresponding monometallic gold material, and can work in solvent-free media. Meanwhile, the high chemoselectivity of gold is preserved.

2. Materials and methods

2.1. Preparation of catalysts

Gold catalysts were synthesised by a deposition-precipitation technique of the gold nanoparticles onto the surface of TiO_2 (Degussa, P-25). The deposition-precipitation procedure was carried out by adding to the support an aqueous solution of $HAuCl_4$ (0.01 M) containing a proper amount of gold. The resulting mixture must be maintained for 2 h at 343 K under vigorous stirring,

* Corresponding author. Fax: +34 96 3877809.
E-mail address: acorma@itq.upv.es (A. Corma).

0021-9517/$ - see front matter © 2009 Elsevier Inc. All rights reserved.
doi:10.1016/j.jcat.2009.04.004

controlling the pH of the solution with NaOH at a specific set point. Then, the resulting powder is filtered, washed with distilled water to remove chlorides, dried in an oven at 373 K, and finally calcined in air at the desired temperature. Depending on the pH of deposition, loading of gold and calcination temperature, gold particles of different sizes and morphologies can be obtained, leading to variable levels of activity [22].

The kinetic work was done with the Au/TiO_2 sample provided by the *World Gold Council* (standard reference catalyst), which contains 1.5 wt% of gold, and this has been synthesised according to the described deposition-precipitation procedure at a pH 7, followed by calcination in air flow at 673 K. In addition, other samples were prepared to obtain catalysts with different levels of activity (see synthesis conditions in Table S1).

Finally, the bimetallic $Au@Pt/TiO_2$ catalysts were prepared by impregnating a proper amount of Pt onto the Au/TiO_2 sample provided by the *World Gold Council*, using H_2PtCl_6 as precursor, followed by a treatment in H_2 flow at 723 K.

2.2. Kinetic experiments

Kinetic measurements were performed in liquid phase using a batch reactor, and the evolution of composition with reaction time was analysed by taking samples at different times on stream. The experiments were carried out in the same reactor (2 ml home-made reinforced glass vial), keeping the volume of the reaction mixture (1 ml) and the stirring rate (1000 rpm) constant, and using always the same amount of catalyst (7.1 mg of the 1.5 wt% Au/TiO_2 sample provided by the *World Gold Council*). In a typical experiment, the catalyst is placed into the reactor together with the reaction mixture. The system is then purged with H_2, before heating up the solution, in order to completely remove the oxygen from the system. Under atmospheric pressure of H_2, the reactor is heated up to the desired temperature, and finally the H_2 pressure is fixed and maintained during all the experiment at a selected set point value. Several samples were taken at different times to have a minimum of three results at conversion levels below 20%. The conversion-time results were fitted to a straight line through the origin, and initial rates were obtained from the slope.

2.3. Isotopic HD exchange experiments

Hydrogen/deuterium (H/D) exchange experiments were carried out in a flow reactor at 298, 348 and 393 K, according to the procedure depicted in [23]. The feed gas consisted of 2 ml/min H_2, 2 ml/min D_2 and 6 ml/min argon, and the total weight of catalyst was 125 mg. Reaction products (H_2, HD and D_2) were analysed with a mass spectrometer (Omnistar, Balzers). Prior to catalytic test, the samples were activated in flowing Argon (10 ml/min) at room temperature (298 K) for 30 min. Then, the gas feed was changed to the reactant gas composition, while the temperature was maintained at 298 K for additional 30 min. At this point, the temperature was increased to 348 K at 10 K/min, maintained for 30 min at that temperature and further increased to 393 K at 10 K/min.

3. Kinetic experiments and models

To study the kinetic behaviour of the Au/TiO_2 system on the hydrogenation of nitroaromatic compounds, we have selected nitrobenzene as a model reactant. Indeed, the kinetics of nitrobenzene hydrogenation into aniline has been widely studied in the literature with metal catalysts such as Pd [24], Pt [25,26], Cu [27] or Ni [28,29], but no references were found for gold-based materials. According to Hougen–Watson/Langmuir–Hinshelwood principles, for describing the mechanism of reactions occurring onto the surface of heterogeneous catalyst [30,31], different rate expressions can be obtained when assuming different reaction steps as the rate-limiting step.

In the case of the hydrogenation of nitroaromatics on Au/TiO_2 catalysts, it has been previously reported that the nitro groups are activated at Au/Ti interphases [21,32], while H_2 dissociatively adsorbs on certain positions of the gold crystals [33]. Considering this previous knowledge, a reduced set of reasonable kinetic equations may be initially proposed as the most probable candidates to match the behaviour of the gold catalyst. These models, which have been summarised in Table 1, involve that both reactants, i.e. nitrobenzene and H_2, are adsorbed onto the surface of Au/TiO_2 before reacting, with the adsorption of H_2 molecules being dissociative. However, it remains to be known if nitrobenzene and H_2 share one unique type of active site or, on the contrary, they adsorb

Table 1
Plausible Hougen–Watson/Langmuir–Hinshelwood models to describe the kinetic behaviour of the nitrobenzene hydrogenation on Au/TiO_2 catalysts.

$r = \frac{k \cdot K_{NB} \cdot K_{H_2} \cdot C_{NB} \cdot P_{H_2}}{(1 + K_{NB} \cdot C_{NB} + \sqrt{K_{H_2} \cdot P_{H_2}})^3}$	(1)	**Control of the surface reaction** NB and H_2 react after adsorbing on active sites with the same nature (competitive adsorption)
$r = \frac{k \cdot K_{NB} \cdot K_{H_2} \cdot C_{NB} \cdot P_{H_2}}{(1 + K_{NB} \cdot C_{NB}) \cdot (1 + \sqrt{K_{H_2} \cdot P_{H_2}})^2}$	(2)	**Control of the surface reaction** NB and H_2 react after adsorbing on active sites with different nature
		Control of the surface reaction NB and H_2 react after adsorbing on active sites with different nature
$r = \frac{k \cdot K_{NB} \cdot K_{H_2} \cdot C_{NB} \cdot P_{H_2}}{\left(1 + K_{NB} \cdot C_{NB} + \sqrt{K'_{H_2} \cdot P_{H_2}}\right) \cdot (1 + \sqrt{K_{H_2} \cdot P_{H_2}})^2}$	(3)	In addition, H_2 also adsorbs on the same active site as NB
$r = \frac{k \cdot K_{NB} \cdot K_{H_2} \cdot C_{NB} \cdot P_{H_2}}{(1 + K_{NB} \cdot C_{NB}) \cdot (1 + \sqrt{K_{H_2} \cdot P_{H_2}} + K'_{NB} \cdot C_{NB})^2}$	(4)	In addition, NB also adsorbs on the same active site as H_2
$r = \frac{k_{H_2} \cdot P_{H_2}}{(1 + K_{NB} \cdot C_{NB})^2}$	(5)	**Control of the adsorption/dissociation of H_2** NB and H_2 react after adsorbing on active sites with the same nature, but the H_2 dissociation is the limiting step of the reaction
$r = \frac{k_{NB} \cdot C_{NB}}{(1 + \sqrt{K_{H_2} \cdot P_{H_2}})}$	(6)	**Control of the adsorption/dissociation of NB** NB and H_2 react after adsorbing on active sites with the same nature, but the NB adsorption is the limiting step of the reaction

[*] k = kinetic constant of the surface reaction; k_{H2} = kinetic constant of the H_2 dissociation; k_{NB} = kinetic constant of the nitrobenzene adsorption; K_{H2} = adsorption constant of H_2 in the equilibrium; K_{NB} = adsorption constant of nitrobenzene in the equilibrium.
[**] C_{NB} = concentration of nitrobenzene; P_{H2} = pressure of H_2.

on different sites (with a different nature, e.g. on the top of gold nanoparticles or at Au/Ti interphases), and moreover which step of the process (surface reaction, adsorption of any reactant, etc.) is limiting the global reaction rate. According to the mathematical formulation of the models in Table 1, it is possible to predict the evolution of the initial reaction rate with the initial concentration of nitrobenzene and initial pressure of H_2 for each of the potential mechanisms. Figure S1 in Supplementary Online Material graphically shows these trends, which will facilitate discrimination among the different potential mechanisms by comparing the real experimental results with the theoretical curves.

We have considered a specific range of working conditions for the kinetic study taking into account feasible industrial conditions [34,35], previous literature on the field [7,24–29] and our knowledge about the behaviour of Au/TiO_2 catalysts [1,21,32]. This space of research is shown in Table S2, where the range of process variables studied, i.e. concentration of substrate (C_{NB}), H_2 pressure (P_{H2}) and reaction temperature (T), has been presented.

4. Results and discussion

4.1. Kinetic study

4.1.1. Influence of the concentration of nitrobenzene on the reaction rate

From the kinetic equations presented in Table 1, it is possible to infer that the effect of the initial nitrobenzene concentration on the initial hydrogenation rate should allow an easy discrimination between models 2–3–6 and models 1–4–5, since the former group of expressions involve a continuous increase in the initial reaction rate with C_{NB}, while the latter group involve a decrease in the initial rate of hydrogenation over a certain initial concentration of the nitroaromatic compound. Thus, initial reaction rates were measured at different C_{NB} levels under "constant" H_2 pressure and temperature (Fig. 1). It can be observed that for highly diluted reaction mixtures the initial reaction rate rapidly increases when the concentration of nitrobenzene increases up to a maximum (r_0 = 0.31 mmol/h at C_{NB} = 0.198 mmol/l), and then decreases when increasing further the concentration of nitrobenzene. This kinetic behaviour for C_{NB} > 0.198 mmol/l, which is the preferred range of nitrobenzene concentration from a process point of view, cannot be reproduced by models 2, 3 and 6 (see the reference curves for each model in Figure S1). On the contrary, models 1 and 4, which correspond to a competing adsorption between H_2 and nitrobenzene in one unique type of active sites, or model 5 controlled by adsorption/dissociation of H_2 at higher C_{NB} values, could properly fit the experimental results within the most interesting range of C_{NB} (0.4–1.2 mmol/l). Up to this point, three-reaction models, i.e. 1, 4 and 5, could fit the experimental results, and further work is required to discriminate among them.

4.1.2. Influence of H_2 pressure

Eqs. (1) and (4) could be easily distinguished from 5 by evaluating the effect of hydrogen pressure (P_{H2}) on the initial reaction rate (r_0) [30,31], since a non-lineal increase of the reaction rate (asymptotic or parabolic) should be observed for the surface reaction control (models 1 and 4), whereas a linear increase should be observed if the dissociation of H_2 is the limiting step (model 5). Therefore, new experiments were performed at variable initial hydrogen pressures (from 2 to 12 bar), keeping the concentration of nitrobenzene (0.418 mmol/l), the reaction temperature (393 K) and the amount of catalyst (7.1 mg) constant. When initial reaction rates at different P_{H2} are plotted in Fig. 2, a linear increase in the initial reaction rate can be seen when increasing the H_2 pressure within the range of pressures studied here. This kinetic behaviour indicates that, at least for high concentrations of nitrobenzene, the adsorption/dissociation of H_2 is the controlling step of the reaction (see curves of reference for each model 5 in Figure S1).

We have decided to confirm the conclusion previously achieved through a classical Hougen–Watson/Langmuir–Hinshelwood kinetic approach, by measuring the rate of H_2–D_2 exchange with the previous catalyst as well as with a series of Au/TiO_2 catalysts showing different activities for the hydrogenation of nitroaromatics. Thus, several Au/TiO_2 samples were prepared under variable synthesis conditions (see Section 3), leading to catalysts with different activity levels. We could assume that if a direct correlation between the rate of hydrogenation and the rate of H_2–D_2 exchange is observed, it will be a confirmation that for Au/TiO_2 catalysts the hydrogenation of nitroaromatics is indeed controlled by H_2 dissociation. Results from Fig. 3 show a linear correlation between the rate of H_2–D_2 exchange for the different Au/TiO_2 catalysts and their activity to reduce 3-nitrostyrene, confirming that the reaction is controlled by H_2 dissociation on gold, and that model 5 represents the kinetic behaviour (see Supplementary Material for the elucidation of the related equation from the elemental reaction steps).

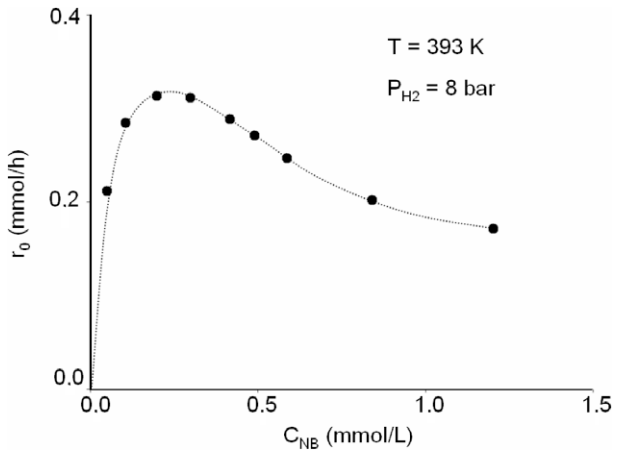

Fig. 1. Influence of the concentration of nitrobenzene on its initial hydrogenation rate at a constant reaction temperature (393 K), constant H_2 pressure (8 bar) and constant amount of the Au/TiO_2 catalyst (7.1 mg). Initial reaction rates were always calculated at conversion levels inferior to 15%.

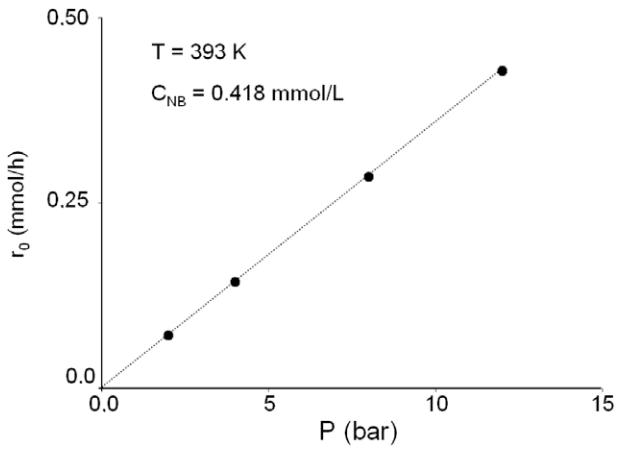

Fig. 2. Influence of the H_2 pressure on the nitrobenzene hydrogenation rate at a fixed reaction temperature (393 K), fixed concentration of nitroaromatic compound (0.418 mmol/l) and fixed amount of the Au/TiO_2 catalyst (7.1 mg).

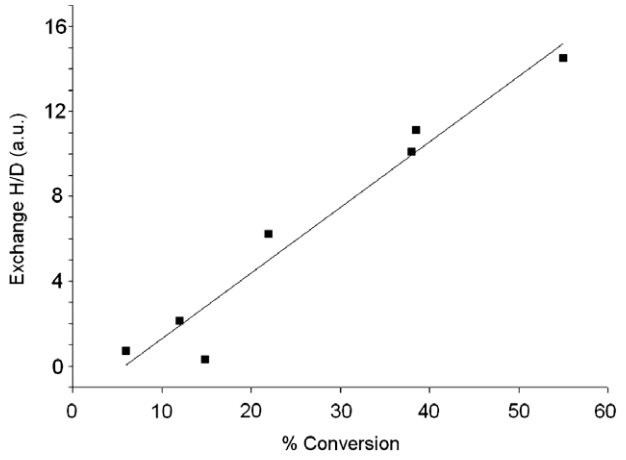

Fig. 3. Relationship between the conversion of nitroaromatic compound (hydrogenation of 3-nitrostyrene) and the isotopic H/D exchange results for a series of Au/TiO_2 catalysts with different levels of activity.

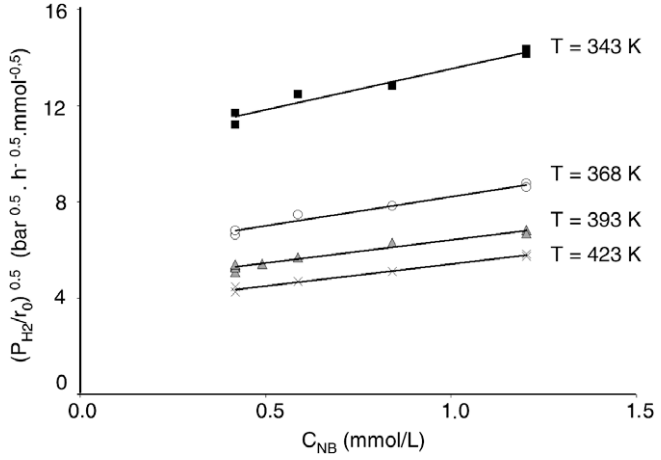

Fig. 4. Catalytic results during the hydrogenation of nitrobenzene with Au/TiO_2 catalysts at different conditions of H_2 pressure, nitrobenzene concentration and reaction temperature, taking into account the linearised expression of model 5.

4.1.3. Calculation of kinetic parameters

A final design of 24 kinetic assays at different C_{NB}, P_{H2} and T values was completed to calculate the parameters for model 5 (Tables S3 and S4). Kinetic results have been fitted to model 5, conveniently linearised (see Fig. 4). It can be observed that the correlation between the experimental and calculated results is good, indicating that the proposed model is suitable to predict the behaviour of the Au/TiO_2 catalysts for hydrogenating nitroaromatic compounds. Then, from the values of the slope ($K_{NB}/k_{H2}^{0.5}$) and the ordinate at the origin ($1/k_{H2}^{0.5}$), the kinetic rate constant for H_2 dissociation (k_{H2}) and the adsorption equilibrium constant of nitrobenzene (K_{NB}) are obtained at different reaction temperatures

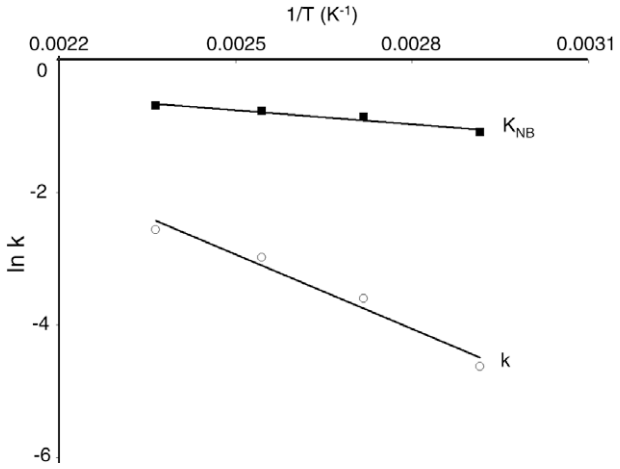

Fig. 5. Influence of the reaction temperature on the kinetic parameters k and K_{NB} (model 5), taking into account the linearised expression of Arrhenius and Van't Hoff equations, respectively.

Table 3
Influence of the reaction temperature on the kinetic parameters of the nitrobenzene hydrogenation with Au/TiO_2 catalysts.

	Linearised Arrhenius/Van't Hoff equation			E_a (KJ/mol)	A^a
	Slope	Ordinate at origin	r^2		
k	−3700,6	6.3	0.96	30.8	561.8
K_{NB}	−709.4	1.0	0.95	5.9	2.8

[a] The same unities as k (mmol bar^{-1} h^{-1}) and K_{NB} (l mmol^{-1}).

(see Table 2). The true activation energy for the kinetic constant and the enthalpy of the nitrobenzene adsorption were calculated according to Arrhenius and Van't Hoff equations (see Fig. 5), respectively, and the results are given in Table 3. The true activation energy measured in this work (31 KJ/mol) is in agreement with the values proposed by other authors on gold-catalysed hydrogenations (36 KJ/mol for the reduction of crotonaldehyde with Au/TiO_2 catalysts [36], 36 KJ/mol for reduction of butadiene with Au/Al_2O_3 catalysts [37]), and is close to the activation energies determined for the H_2–D_2 exchange on Au/Al_2O_3 [38]. On the other hand, the slightly endothermic character of the nitrobenzene adsorption (~6 KJ/mol) has to be highlighted upon, as evidenced by the increase of K_{NB} as the reaction temperature increases. Although this phenomenon, involving an increase of the adsorbed $-NO_2$ species with the temperature, is not very usual in gas-phase reactions, the endothermic behaviour is sometimes observed when working with solid/liquid systems, since the adsorbant–adsorbate interactions can be slightly influenced by additional solvent–adsorbate and solvent–adsorbent interactions [39].

4.2. Designing a catalyst of higher activity

From the performed kinetic study, we can extract relevant conclusions about the Au/TiO_2 system mode of action, and how to in-

Table 2
Catalytic results at different conditions of H_2 pressure, nitrobenzene concentration and reaction temperature for the hydrogenation of nitrobenzene with Au/TiO_2 catalysts (r^2 corresponds to the linear regression coefficient).

T (K)	Linearised Model 5 (Eq. 7)			$k_{H_2} \times 10^2$ (mmol bar^{-1} h^{-1})	$K_{NB} \times 10^2$ (l mmol^{-1})
	Slope	Ordinate at origin	r^2		
343	3.4	10.1	0.96	0.97	33.7
368	2.4	5.8	0.97	3.0	42.1
393	1.9	4.5	0.97	5.1	46.1
423	1.8	3.6	0.99	7.7	50.3

Table 4
Catalytic results during the hydrogenation of 3-nitrostyrene using different Au and Pt catalysts. Feeding composition: 90.5% Toluene, 8.5%3-nitrostyrene, 1% o-xilene (% mol).

Catalyst	T_r (K)	P_{H2} (bar)	% Au[a] (mol)	% Pt a (mol)	Time (h)	% Conversion	% Selectivity[b]	TOF[c]
1.5% Au/TiO_2	393	8	0.23	–	6	98.5	95.9	173
0.2% Pt/TiO_2	313	2	–	0.31	6.5	95.1	93.1	60
1.5% Au/TiO_2	358	8	0.23	–	9	97.8	96.2	70
0.2% Pt/TiO_2	358	8	–	0.31	0.25	95.1	69.7	1380
1.5%Au@0.01%Pt/TiO_2	358	8	0.23	0.0155	0.52	94.5	93.4	550
0.01% Pt/TiO_2	358	8	–	0.0155	6	25.3	48.4	2994

[a] mol metal/mol nitroaromatic × 100.
[b] Selectivity to 3-vinylaniline.
[c] TOF measured as mol converted mol $metal^{-1}$ h^{-1}.

crease the production during the chemoselective hydrogenation of nitroaromatic compounds. For instance, taking into account the kinetic curves (see Figs. 1 and 2) one could work with low concentrations of nitrobenzene and high H_2 pressures. However, this would require increasing the ratio of solvent/reactant. On the contrary, from a practical point of view, it would be desirable to minimise the use of solvents during the manufacture of substituted anilines in order to (1) increase the productivity for a given reactor size, (2) reduce the number of separation operations and (3) reduce the formation of potential wastes. Also, low H_2 pressures would be preferred to simplify the design of equipments and to reduce operation costs. Thus, since the reaction is limited by the amount of H_2 activated on the surface of the catalyst on low-coordinated atoms at the surface of the gold nanoparticles [33], one could prepare catalysts with a larger number of smaller gold crystallites and with proper crystal shapes. While this is certainly a possibility, we thought that, within our means, it would be difficult to selectively increase the number of defects on the exposed gold domains. Therefore, we have taken a second approach to increase the rate of H_2 dissociation on the catalyst, as will be described below.

Recently, we have shown [40] that by using a more active metal such as Pt, and when properly supported and activated on TiO_2, it is possible to perform the chemoselective hydrogenation of 3-nitrostyrene at milder reaction temperatures and H_2 pressures that with Au/TiO_2 catalysts. Unfortunately, TOF values (mol converted mol $metal^{-1}$ h^{-1}) provided by the reported Pt/TiO_2 solid at 313 K and 3 bar of H_2 are low, and the selectivity of this catalyst is partially lost when increasing the reaction temperature to increase TOF (see Table 4 and Table S5). To overcome this situation, we thought to introduce Pt, which can rapidly dissociate H_2, on an Au/TiO_2 catalyst, which has been shown to be much more chemoselective. Although the amount of Pt introduced should be high enough to have an impact on the H_2 dissociation, it should be relatively low to avoid the unselective effects of Pt for hydrogenating substituted nitroaromatics. To do this, we have prepared a series of new catalysts based on the 1.5% Au/TiO_2 catalyst doped with increasing amounts of Pt from 50 to 2000 ppm. Results in Fig. 6 show that while activity of these Au@Pt/TiO_2 catalysts for the hydrogenation of 3-nitrostyrene, measured as TOF, increases when increasing Pt content, the chemoselectivity to reduce the nitro group decreases for Pt contents over 100 ppm (see Table S5 for a detailed distribution of reaction products). Moreover, this result has been compared in Table 4 with a catalytic system containing 100 ppm of Pt but no gold. The low-hydrogenation rate observed in the latter case indicates that even if such small amount of Pt is key to rapidly dissociate H_2, the presence of gold remains necessary to promote the hydrogenation of the nitro group. Then, the final 1.5%Au@0.01%Pt/TiO_2 catalyst maintains excellent levels of selectivity at high conversion levels (see Table 4), while its high activity allows completing the hydrogenation of 3-nitrostyrene in 30 min, instead of the 9 h needed by the Au/TiO_2 system (see Fig. 7 for a comparison between the kinetic behaviour of different catalysts at their respective optimised reaction conditions). In addition, we have checked that, contrary to the Au/TiO_2 catalyst, the hybrid 1.5%Au@0.01%Pt/TiO_2 system can efficiently work in solvent-free media (Fig. 8), which is important for a sustainable process.

Unfortunately, the use of only 0.01% Pt for enhancing the activity of the gold catalyst, while maintaining high chemoselectivity, makes really hard to accurately characterise the distribution of Pt species on the surface of the support, applying either spectroscopic

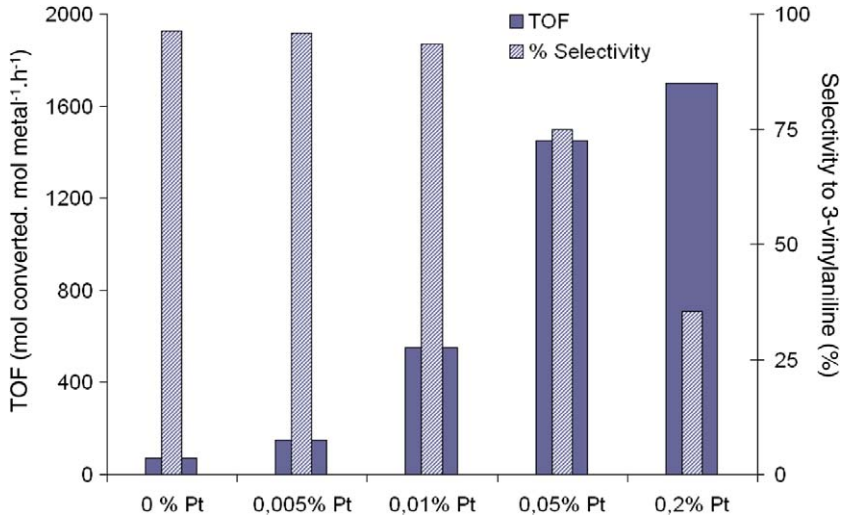

Fig. 6. Influence of the Pt content in the 1.5% Au/TiO_2 catalyst on the TOF values and selectivity towards 3-vinylaniline during the hydrogenation of 3-nitrostyrene.

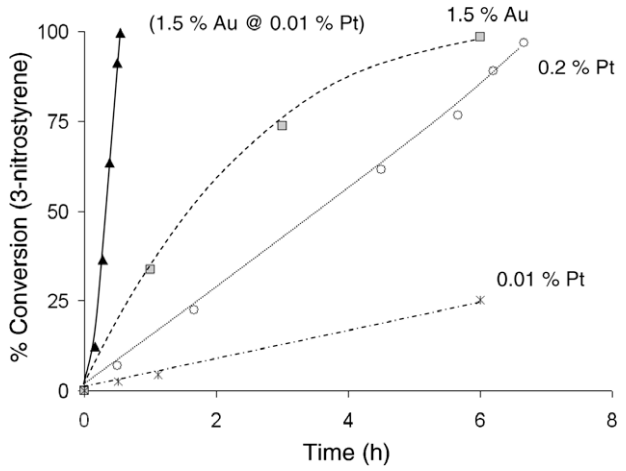

Fig. 7. Evolution of 3-nitrostyrene conversion with reaction time using different supported Au and Pt catalysts (optimised reaction conditions for each type of material, see Table 4).

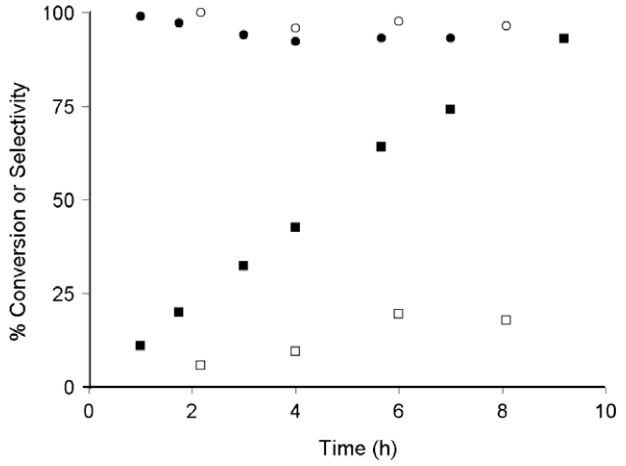

Fig. 8. Evolution of the 3-nitrostyrene conversion (squares) and selectivity to 3-vinylaniline (circles) with reaction time, using a 1.5% Au/TiO_2 catalyst (World Gold Catalyst, white symbols) and the 1.5%Au@0.01%Pt/TiO_2 system (black symbols) under solvent-free reaction conditions. Reaction conditions: 358 K, 8 bar of hydrogen, 100 mg of catalyst.

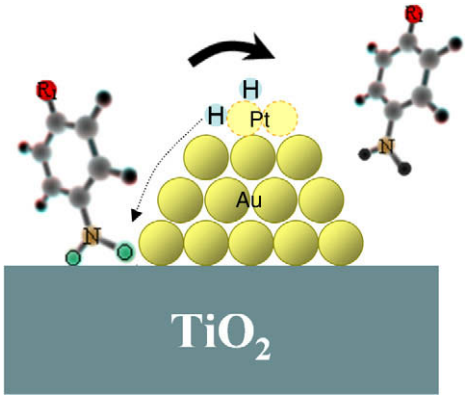

Fig. 9. Plausible scenario to understand the high activity and chemoselectivity shown by the bimetallic 1.5%Au@0.01%Pt/TiO_2, as suggested by catalytic observations. Nitroaromatic compounds are selectively adsorbed at Au–Ti boundaries, while activated hydrogen species are rapidly provided by the Pt sites.

or microscopic techniques. However, we have observed that such increase in the activity using the 1.5%Au@0.01%Pt/TiO_2 catalyst only occurs when the sample is reduced at high temperatures (the same effect is not observed, for instance, by reducing the catalyst at 373 K or using an organic reducing agent). In addition, we have also checked that no increase in the activity is produced by simply reducing the Au/TiO_2 sample (without Pt) at high temperatures. Thus, we can hypothesise that the formation of bimetallic Au@Pt particles during the thermal treatment, favoured at high-reduction temperatures by migration of single Pt atoms along the surface of the support, is essentially responsible for the special catalytic behaviour of the sample. Accordingly, a plausible scenario has been graphically depicted in Fig. 9 in order to easily understand the 1.5%Au@0.01%Pt/TiO_2 mode of action. Unfortunately, we cannot provide any direct evidence of this phenomenon, and further efforts for accurately characterising the catalyst surface should be carried out.

5. Conclusion

Kinetic and isotopic studies for the hydrogenation of nitroaromatics have allowed to find that the rate-controlling step is the dissociation of H_2 on gold. The information obtained in this part of the work has allowed to design a new bimetallic catalyst with an optimised Pt content. The presence of Pt on the bimetallic catalyst increases the rate of H_2 dissociation resulting in a solid that is almost one order of magnitude more active than the monometallic Au/TiO_2, while maintaining high chemoselectivity during the hydrogenation in the presence of other sensitive functional groups.

Acknowledgments

We thank the Spanish government (Project MAT 2006-14274-C02-01), and PROMETEO Project of Generalitat Valenciana.

Appendix A. Supplementary material

Supplementary data associated with this article can be found, in the online version, at doi:10.1016/j.jcat.2009.04.004.

References

[1] A. Corma, P. Serna, Science 313 (2006) 332.
[2] A. Grirrane, A. Corma, H. García, Science 322 (2008) 1661.
[3] R.F. Kovar, F.E. Armond, US Patent 3,975,444 to the US Air Force, 1976.
[4] M. Suchy, P. Winternitz, M. Zeller, WO Patent 91/02278 to Ciba-Geigy, 1991.
[5] J. Butera, J. Bagli, WO Patent 91/09023 to American Home Products, 1991.
[6] A. Burawoy, J.P. Critchley, Tetrahedron 5 (1959) 340.
[7] U. Siegrist, P. Baumeister, H.-U. Blaser, M. Studer, Chem. Ind. Dekker 75 (1998) 207.
[8] H.-U. Blaser, U. Siegrist, H. Steiner, M. Studer, in: R.A. Sheldon, H. van Bekkum (Eds.), Fine Chemicals Through Heterogeneous Catalysis: Aromatic Nitro Compounds, Wiley, New York, 2001, p. 389.
[9] A. Corma, P. Serna, H. García, J. Am. Chem. Soc. 129 (2007) 6358.
[10] F. Porta, L. Prati, M. Rossi, G. Scari, J. Catal. 211 (2002) 464.
[11] M.D. Hughes, Yin-Jun Xu, P. Jenkins, P. McMorn, P. Landon, D.I. Enache, A.F. Carley, G.A. Attard, G.J. Hutchings, F. King, E.H. Stitt, P. Johnston, K. Griffin, C.J. Kiely, Nature 437 (2005) 1132.
[12] T.A. Nijhuis, T. Visser, B.M. Weckhuysen, Angew. Chem. Int. Ed. 44 (2005) 1115.
[13] A.S.K. Hashmi, J.P. Weyrauch, M. Rudolph, E. Kurpejovic, Angew. Chem. Int. Ed. 43 (2004) 6545.
[14] A.S.K. Hashmi, L. Schwarz, J.-H. Choi, T.M. Frost, Angew. Chem. Int. Ed. 39 (2000) 2285.
[15] S. Carrettin, J. Guzman, A. Corma, Angew. Chem. Int. Ed. 44 (2005) 2242.
[16] C. González-Arellano, A. Corma, M. Iglesias, F. Sánchez, Chem. Commun. (2005) 3451.
[17] S. Naito, M. Tanimoto, J. Chem. Soc. Chem. Commun. (1988) 832.
[18] C. Milone, R. Ingoglia, L. Schipilliti, C. Crisafulli, G. Neri, S. Galvagno, J. Catal. 236 (2005) 80.
[19] Y. Ito, M. Sawamura, T. Hayashi, J. Am. Chem. Soc. 108 (1986) 6405.
[20] C. González-Arellano, A. Corma, M. Iglesias, F. Sánchez, Chem. Commun. (2005) 1990.

[21] M. Boronat, P. Concepción, A. Corma, S. González, F. Illas, P. Serna, J. Am. Chem. Soc. 129 (2007) 16230.
[22] M. Haruta, Catal. Today 36 (1997) 153.
[23] E. Bus, J.T. Miller, J.A. van Bokhoven, J. Phys. Chem. B. 109 (2005) 14581.
[24] B. Amon, H. Redlingshöfer, E. Klemm, E. Dieterich, G. Emig, Chem. Eng. Proc. 38 (1999) 395.
[25] V. Höller, D. Wegricht, I. Yuranov, L. Kiwi-Minsker, A. Renken, Chem. Eng. Technol. 23 (2000) 3.
[26] E. Lamy-Pitara, B. N'Zemba, J. Barbier, F. Barbot, L. Miginiac, J. Mol. Catal. A Chem. 142 (1999) 39.
[27] L. Petrov, K. Kumbilieva, N. Kirkov, Appl. Catal. 59 (1990) 31.
[28] F. Turek, R. Geike, R. Lange, Chem. Eng. Process. 20 (1986) 213.
[29] J. Relvas, R. Andrade, F.G. Freire, F. Lemos, P. Araújo, M.J. Pinho, C.P. Nunes, F.R. Ribeiro, Catal. Today 33–135 (2008) 828.
[30] F.F. Froment, K.B. Bischoff, Chemical Rector Analysis and Design, second ed., John Wiley, Berlin, 1990.
[31] J.B. Butt, Reaction Kinetics and Reactor Design, second ed., Marcel Dekker, 1999.
[32] A. Corma, P. Concepcion, P. Serna, Angew. Chem. Int. Ed. 46 (2007) 7266.
[33] A. Corma, M. Boronat, S. González, F. Illas, Chem. Commun. (2007) 3371.
[34] Kirk and Othmer, Encyclopedia of Chemical Technology, vol. 2., second ed., (1967), p. 411.
[35] T. Kahl, K.-W. Schröder, Ullmann's Encyclopedia of Industrial Chemistry, sixth ed., Wiley-VCH, Weinheim, Germany, 2002.
[36] R. Zanella, C. Louis, S. Giorgio, R. Touroude, J. Catal. 223 (2004) 328.
[37] D.A. Buchanan, G. Webb, J. Chem. Soc. Faraday Trans. 71 (1975) 134.
[38] E. Bus, J.T. Miller, J.A. van Bokhoven, J. Phys. Chem. B. 109 (2005) 14581.
[39] J.M. Corkill, J.F. Goodman, J.R. Tate, Trans. Faraday Soc. 62 (1966) 979.
[40] A. Corma, P. Serna, P. Concepción, J.J. Calvino, J. Am. Chem. Soc. 130 (2008) 8748.